

Archived at the Flinders Academic Commons

<http://dspace.flinders.edu.au/dspace/>

*Copyright (2005) American Institute of Physics. This article may be downloaded for personal use only. Any other use requires prior permission of the author and the American Institute of Physics.*

*The following article appeared in* Saha, S., Feng, W., Falzon, C., & Brunger, M.J., 2005. Coexistence of 1,3-butadiene conformers in ionisation energies and Dyson orbitals. *Journal of Chemical Physics*, 123(12), 124315-1-124315-14. *and may be found at* [doi:10.1063/1.2034467](https://doi.org/10.1063/1.2034467)

## Coexistence of 1,3-butadiene conformers in ionization energies and Dyson orbitals

Saumitra Saha, Feng Wang,<sup>a)</sup> and Chantal T. Falzon

Centre for Molecular Simulation, Swinburne University of Technology, P.O. Box 218, Hawthorn, Melbourne, Victoria 3122, Australia

Michael J. Brunger

School of Chemistry, Physics and Earth Sciences, Flinders University, G.P.O. Box 2100, Adelaide, SA 5001, Australia

(Received 9 June 2005; accepted 20 July 2005; published online 28 September 2005)

The minimum-energy structures on the torsional potential-energy surface of 1,3-butadiene have been studied quantum mechanically using a range of models including *ab initio* Hartree-Fock and second-order Møller-Plesset theories, outer valence Green's function, and density-functional theory with a hybrid functional and statistical average orbital potential model in order to understand the binding-energy (ionization energy) spectra and orbital cross sections observed by experiments. The unique full geometry optimization process locates the *s-trans*-1,3-butadiene as the global minimum structure and the *s-gauche*-1,3-butadiene as the local minimum structure. The latter possesses the dihedral angle of the central carbon bond of 32.81° in agreement with the range of 30°–41° obtained by other theoretical models. Ionization energies in the outer valence space of the conformer pair have been obtained using Hartree-Fock, outer valence Green's function, and density-functional (statistical average orbital potentials) models, respectively. The Hartree-Fock results indicate that electron correlation (and orbital relaxation) effects become more significant towards the inner shell. The spectroscopic pole strengths calculated in the Green's function model are in the range of 0.85–0.91, suggesting that the independent particle picture is a good approximation in the present study. The binding energies from the density-functional (statistically averaged orbital potential) model are in good agreement with photoelectron spectroscopy, and the simulated Dyson orbitals in momentum space approximated by the density-functional orbitals using plane-wave impulse approximation agree well with those from experimental electron momentum spectroscopy. The coexistence of the conformer pair under the experimental conditions is supported by the approximated experimental binding-energy spectra due to the split conformer orbital energies, as well as the orbital momentum distributions of the mixed conformer pair observed in the orbital cross sections of electron momentum spectroscopy. © 2005 American Institute of Physics.

[DOI: 10.1063/1.2034467]

### I. INTRODUCTION

Known as a human carcinogen, 1,3-butadiene ( $\text{CH}_2=\text{CH}-\text{CH}=\text{CH}_2$ ) in both rodents and humans might induce tumor formation due to its metabolism to DNA-reactive intermediates resulting in genetic alternations in protooncogenes and/or tumor suppressor genes.<sup>1</sup> More recently, the development of molecular electronics in the area of molecule-based and molecule-controlled electronic device research<sup>2</sup> reveals that intrinsic properties of molecules with conjugated  $\pi$  bonds, such as molecular length, conformation, and the highest occupied molecular orbital (HOMO)-lowest unoccupied molecular orbital (LUMO), i.e., HOMO-LUMO gap, play important roles in this exciting nanomaterials area. As a prototypical example of molecules with conjugated  $\pi$  bonds, 1,3-butadiene exhibits, by virtue of facile rotation about the CC–CC single bond at ambient temperatures, an equilibrium mixture of *s-trans* and higher energy *s-cis/s-gauche*

conformers.<sup>3</sup> Therefore, it is increasingly important to comprehend the electronic structures of 1,3-butadiene conformers in order to provide more confidence in detailed theoretical understanding of the experimental observations.

Experimental evidence of ionization energies of *L*-phenylalanine<sup>4</sup> revealed that the conformer-dependent ionization energy (lowest ionization state) could range from 8.80 to 9.15 eV. In fact, the results of photoelectron spectroscopy<sup>5</sup> (PES) and electron momentum spectroscopy<sup>4</sup> (EMS) of 1,3-butadiene cannot be satisfactorily interpreted using the global minimum structure of *s-trans*-1,3-butadiene alone, indicating appearance of other conformers under the experimental conditions. For many molecules, energy barriers for the conformational changes are rather high so that they tend to be found in only one conformer form. However, for moderate energy barriers, some such conformers would overcome these barriers during relaxation and adopt more stable forms.<sup>4</sup> The resultant conformer distribution is a complex function of the relative energies of the isomers, barrier heights, temperature, etc, constituting in a Boltzmann distri-

<sup>a)</sup> Author to whom correspondence should be addressed. Electronic mail: fwang@swin.edu.au

bution. Hence, molecules such as 1,3-butadiene are dominantly presented in their most stable canonical forms, but they may configure different conformers by rotating around the CC–CC single bond in 1,3-butadiene under certain conditions. As a result, the determination of torsional potentials around the CC–CC single bond in 1,3-butadiene and conjugated systems is still an active research area.<sup>7</sup> Although the global minimum structure of the most stable conformer was established as a planar *s-trans* structure (here *s* indicates that the species rotates around the single bond), in studies such as Refs. 7–12 and references therein the view of interconversion or coexistence of the planar *s-trans* conformer and non-planar *s-gauche*-1,3-butadiene conformer of the less stable local minimum structure has received strong support from experimental evidence.<sup>3,5,6</sup>

Both such structures of the conformer pair are almost identical in their geometries except for the dihedral angle formed by the four-carbon frame: C=C–C=C, where the *s-trans* conformer exhibits a dihedral angle of 180°, whereas the planar *s-cis* conformer possesses an angle of 0°. It was predicted theoretically that the dihedral angle of the *gauche* conformer of 1,3-butadiene lies in the range of 30°–41°,<sup>7</sup> depending on the model employed. The experimental value is believed to be 43°. <sup>13</sup> Unfortunately, almost no experiment is particularly sensitive to such a dihedral angle, as “the energy difference between 0° and ±15° would then be expected to be so small that the zero-point torsional level would probably lie above the potential energy for the planar geometry, making a strictly geometric distinction almost meaningless.”<sup>14</sup> However, this statement may not be true if experimental techniques could be developed to measure other properties, such as the vibrational transition moment angles (VTMA) technique,<sup>15</sup> rather than the traditional energetic properties. In addition, as pointed out in Ref. 16, it may not be a very meaningful practice to compare the conformer stability if the energetics have very subtle differences and if there is a lack of experimental evidence at the individual (isolated) conformer level. Moreover, the theoretical energy differences among conformers could be very small and, in some cases, may be well within the errors introduced by the models employed.

In this paper, we will concentrate on information which could differentiate the conformers, such as energies, dipole moments, orbital charge distributions, and orbital momentum distributions, of the *s-trans/s-gauche* 1,3-butadiene conformers using the recently developed technique known as dual space analysis (DSA).<sup>17</sup> That is, structures of the conformers were studied using a variety of quantum-mechanical methods, including *ab initio* (RHF, MP2), density-functional theory (DFT), B3LYP and SAOP, and outer valence Green’s function (OVGF) method. The Dyson orbitals of the conformers were then mapped into momentum space directly to give orbital momentum distributions, using the independent particle picture<sup>18,19</sup> and plane-wave impulse approximation (PWIA).<sup>20</sup> The information obtained from both the coordinate and momentum spaces helped in the analysis and synthesis of the orbitals to reproduce the experimental findings, so that a more comprehensive orbital-based understanding of the conformers could be achieved.

## II. METHODS AND COMPUTATIONAL DETAILS

Organic conformers might differ from only small energetic discrepancies, but they have profound differences in their spatial and anisotropic properties as well as reactivity. This brings challenges to energy-dominant experimental measurements, such as PES, due to limitations such as instrumental resolution. However, techniques which utilize momentum might probe the significant differences exhibited by conformers. As a result, DSA,<sup>17</sup> a combined method for processing information from coordinate and momentum spaces such as energies and orbital momentum distributions (MDs), has been demonstrated to be capable of providing a unique, novel, and comprehensive means to study conformers unambiguously.<sup>21–24</sup>

The geometry optimization and ionization energy calculations of *s-trans/s-gauche*-1,3-butadiene were performed using various quantum mechanical methods. In coordinate space, *ab initio* methods such as RHF/TZVP and MP2/TZVP were employed for comparison purposes, the hybrid DFT model of B3LYP/TZVP has also been employed to determine the geometries of the conformers with  $C_{2h}$  (*s-trans*) and  $C_2$  symmetry (*s-gauche*) for consistency. The TZVP basis set is a reasonably large triple zeta with valence polarized (TZVP) basis set due to Godbout *et al.*<sup>25</sup> The outer valence Green’s function method, OVGF/TZVP, was also employed to generate outer valence orbital ionization energies and their corresponding spectroscopic pole strengths for each conformer. Such independent calculations provide information and help assess the approximations applied in the present study. All the above electronic calculations were performed using both the GAMESS-US02 (Ref. 26) and GAUSSIAN03 (Ref. 27) packages of computational chemistry programs, with the OVGF/TZVP calculations being performed using GAUSSIAN03 (Ref. 27) only.

An important goal of the present study is to interpret an earlier EMS experimental orbital cross section,<sup>6</sup> which likely produced the information on the stable conformers of 1,3-butadiene including the *s-gauche* conformer (local minimum structure). That is, to study electronic structural information of the minimum structures of the species, *s-trans*-1,3-butadiene and *s-gauche*-1,3-butadiene. The other distinct structures on the torsional potential-energy surface, such as the energy barrier between the global and local minima, as well as the *s-cis* saddle-point configuration, possess higher energies. As a result, the probabilities of these structures being observed in the EMS measurements under the experimental conditions<sup>6</sup> are very small based on Boltzmann distributions. In addition, the approach employed in the present study is not particularly sensitive to details of the torsional angles in the vicinity of the *s-gauche* conformer to discern the *s-gauche* and *s-cis* conformers (refer to Ref. 28) except for the molecular electrostatic potentials [MEP, see Figs. 1(b) and 1(c)]. Therefore, this study focuses on the conformers with minimum-energy structures on the torsional potential-energy surface of 1,3-butadiene.

DFT-calculated orbital energies have traditionally been found to be in poor agreement with experimental binding-

TABLE I. Optimized geometries of 1,3-butadiene using the B3LYP/TZVP models, together with other theoretical calculations and available experiments.

Geometry	<i>s-trans-C<sub>2h</sub></i>			<i>s-gauche-C<sub>2</sub></i>		
	This work	Other theory <sup>a</sup>	Expt. <sup>b</sup>	This work	Other theory <sup>a</sup>	Other theory <sup>c</sup>
$R_{C=C}/\text{\AA}$	1.34	1.34	1.34	1.34	1.34	1.34
$R_{C-C}/\text{\AA}$	1.46	1.46	1.47	1.47	1.47	1.47
$R_{C(3)}-R_{C(5)}/\text{\AA}$	1.08	1.09	1.09	1.08	1.09	1.09
$R_{C(3)}-R_{C(7)}/\text{\AA}$	1.09	1.08	1.09	1.08	1.09	1.09
$R_{C(1)}-R_{C(9)}/\text{\AA}$	1.09	1.09	1.09	1.09	1.09	1.09
$\angle C_{(1)}C_{(2)}C_{(4)}/^\circ$	124.27	123.73	122.8	125.87	124.12	124.1
$\angle H_{(8)}C_{(4)}C_{(2)}/^\circ$	121.34	121.41	119.5	121.80	121.33	121.3
$\angle H_{(6)}C_{(4)}C_{(2)}/^\circ$	121.60	121.77	119.5	121.28	121.58	121.6
$\angle H_{(10)}C_{(2)}C_{(1)}/^\circ$	116.51	116.71	117.7 <sup>d</sup>	115.57	116.87	116.9
$\angle C_{(4)}C_{(2)}C_{(1)}C_{(3)}/^\circ$	180.00	180.00	...	32.81 <sup>e</sup>	37.81	37.8
$\angle H_{(6)}C_{(4)}C_{(2)}C_{(1)}/^\circ$	180.00	180.00	...	179.02	178.48	178.5
$\angle H_{(8)}C_{(4)}H_{(6)}/^\circ$	117.06	...	...	116.91	...	...
$\angle C_{(4)}C_{(2)}H_{(10)}/^\circ$	119.23	...	...	118.55	...	...
$\angle H_{(6)}H_{(8)}C_{(4)}C_{(2)}/^\circ$	180.00	...	...	179.13	...	...
$\angle H_{(8)}C_{(4)}C_{(2)}H_{(10)}/^\circ$	180.00	...	...	176.55	...	...

<sup>a</sup>Reference 41.<sup>b</sup>The sector electron-diffraction (ED) method (Refs. 41 and 44).<sup>c</sup>Reference 42.<sup>d</sup>Calculated from two adjacent angles (Ref. 41).<sup>e</sup>The MP2/TZVP//MP2/TZVP model of the present work gives 39.10°.

-energy measurements, as Koopmans' theorem does not hold for Kohn-Sham orbital energies. However, recent developments in DFT using the "meta-Koopmans" theorem, an analog of Koopmans' theorem for DFT,<sup>29-31</sup> can generate vertical ionization energies of molecular species with an accuracy up to 0.2 eV.<sup>32</sup> This is achievable using the recently developed density-functional method, the statistical average of different model orbital potentials (SAOP),<sup>33-35</sup> which is embedded in the Amsterdam Density Functional (ADF) suite of programs.<sup>36</sup> In addition to the binding energies calculated using Koopmans theorem (RHF) and the Green's function, OVGf, the present work also computed binding energies using the SAOP/TZ2P model. Here the TZ2P basis set is a Slater-type triple zeta plus double polarization basis set,<sup>37</sup> which is the closest basis set to the Gaussian-type TZVP basis set. The geometrical initial guesses for the carbon backbone were based on four distinct structures of normal butane<sup>22</sup> without any assumptions of either planarity or C-C bonds (double or single).

The ionization energies of the outer valence space using RHF/TZVP, OVGf/TZVP, as well as the SAOP/TZ2P models were all based on the optimized geometries of B3LYP/TZVP for consistency, unless otherwise indicated. For wavefunction generation, due to technical reasons,<sup>17</sup> additional single-point calculations based on the optimized geometries of the conformers, i.e., B3LYP/TZVP//B3LYP/TZVP, have been performed for the molecular wave functions. They were then Fourier transformed into  $\mathbf{k}$ -space and under the Born-Oppenheimer approximation, independent particle description, and PWIA,<sup>20</sup> the momentum distribution (MD,  $\sigma$ ) is given by

$$\sigma \propto \int d\Omega |\psi_j(\mathbf{k})|^2, \quad (1)$$

which is proportional to the momentum space one-electron Dyson orbital  $\psi_j(\mathbf{k})$ . Dyson orbitals represent the changes in electronic structure accompanying the detachment of an electron from a molecule.<sup>38</sup> Corresponding to each ionization energy in the DFT calculations, the Dyson orbitals are proportional to canonical, Kohn-Sham (KS) orbitals.<sup>39</sup> The simulation procedure for orbital momentum distributions of the 1,3-butadiene conformers was based on the experimental conditions of a previous EMS study.<sup>6</sup>

### III. RESULTS AND DISCUSSION

#### A. Property correlation between *s-trans/s-gauche*-1,3-butadiene

Two minimum structures of 1,3-butadiene were found, one was the global minimum structure with a planar  $C_{2h}$  symmetry ( $X^1\Sigma^+$ ), the other was the local minimum structure of *s-gauche* ( $C_2$ ) with the CC-CC dihedral angle of 32.81°, deviating from the planar *cis*-1,3-butadiene structure ( $\delta = 0^\circ$ ). This result agrees well with previous studies for the *s-gauche* conformer of 1,3-butadiene as the local minimum structure. In a recent study,<sup>7</sup> this dihedral angle was given in the range of 30°-41°, depending on the model employed. For example, the B3LYP/cc-pVDZ model gave the dihedral angle of 30°, whereas the RHF/aug-cc-pVDZ model gave an angle of 41°.<sup>7</sup> An experimental value for this angle was 43°.<sup>13</sup>

The most significant geometrical difference between *s-trans/s-gauche*-1,3-butadiene is due to the rotation of the central C-C bond, i.e., the CC-CC dihedral angle, resulting in a very small energy variation. Table I compares the geo-



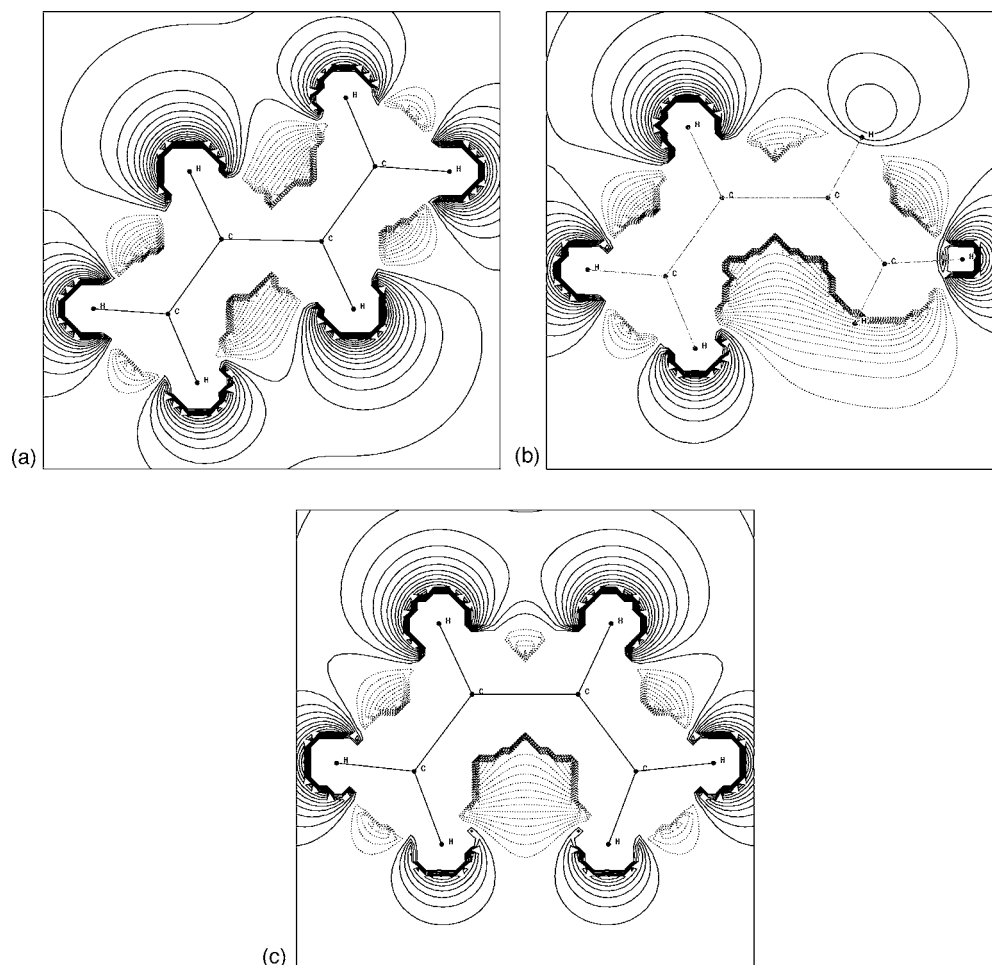


FIG. 1. Molecular electrostatic potentials (MEP) of (a) *s-trans*-1,3-butadiene, (b) *s-gauche*-1,3-butadiene, and (c) *s-cis*-1,3-butadiene.

metrical parameters of *s-trans/s-gauche* 1,3-butadiene, as well as other theoretical studies and available electron-diffraction (ED) experimental data. It is seen that the *s-trans/s-gauche*-1,3-butadiene conformers have no fundamental geometrical differences in the C=C and C–H bond lengths, which are consistent with other studies such as Refs. 40–42. The bond angles and dihedral angles between the two conformers differ only to reflect the *s-gauche* structure in the table. The double C=C bonds, with a bond length of 1.34 Å in the present study, which is slightly longer than a typical C=C double bond in isolated ethene (1.33 Å) in the gas phase, agrees well with the ED experiment.

The most interesting and geometrically noticeable bond length of the conformers is the central C–C “single bond.” The present study, using different models, produced a bond length between 1.456 and 1.460 Å. The B3LYP/TZVP model gave a value of 1.456 Å for the *s-trans*-1,3-butadiene conformer, which is in good agreement with 1.456 Å obtained using the MP2/6-31G\* model<sup>41</sup> and 1.457 Å using the B3LYP/6-31G\*\* model.<sup>43</sup> The ED experimental values for this bond length, however, consistently suggested a longer bond length of 1.467,<sup>44</sup> 1.463,<sup>45</sup> and 1.467 Å. (Note that the experiment in Ref. 46 treated the sample as a coexisting mixture of *s-trans/s-cis* or *s-gauche* conformers of 1,3-butadiene). This experimental bond length is obviously longer than the predicted C–C bond for the *s-trans* con-

former. Coincidentally, this experimental CC–CC bond length is surprisingly close to the C–C bond length of the *s-gauche* species predicted by the present model (B3LYP/TZVP) as well as other models such as MP2/6-31G\* (Refs. 41 and 42) of 1.468 Å and B3LYP/6-31G\*\* (Ref. 43) of 1.471 Å. As a single bond, the bond length here is much shorter than an isolated single bond in ethane (1.530 Å), using the same model (B3LYP/TZVP), indicating its transition nature between a C=C double bond (1.330 Å for the isolated C=C bond in ethene) and a C–C single bond. The unexpectedly long central C–C bond length of 1,3-butadiene observed by experiment suggests the coexistence of the *s-gauche* conformer under the experimental condition, so that the experiments likely observed the C–C bond length of *s-gauche*-1,3-butadiene at that instance.

MEP show the distribution of electronic charge on the molecule and give a good idea of the shape of the molecule. As MEP correlates with dipole moment, electronegativity, and partial charges, it provides a visual method to understand the relative polarity of a molecule. Figure 1 shows the MEP as mapped onto the electron charge density of the conformers. The contour pattern represents the charge distribution. In this case, the solid contours represent the most positively charged regions, and the dot contours show the most negatively charged regions. As one might predict, the negative

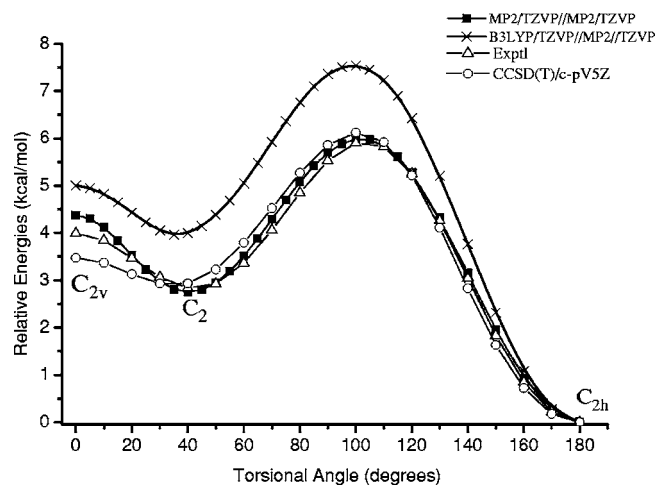


FIG. 2. Cross sections on the torsional potential-energy curve of 1,3-butadiene as a function of the torsional angle  $\delta$ . The energies at  $\delta=180^\circ$  are normalized to zero for all relative energies. The models MP2/TZVP//MP2/TZVP and B3LYP/TZVP//MP2/TZVP calculated the torsional potential energies based on the single-point calculations of MP2/TZVP and B3LYP/TZVP, respectively, in which the geometries were fixed at the optimized geometry of *s-trans*-1,3-butadiene obtained using the MP2/TZVP model, except for the CC-CC torsional angle.

charge is found mostly around the carbon atoms, and the more positive regions are found near the hydrogen atoms. For the case of the *s-trans* conformer, the distribution of the MEP is symmetric, but the central  $C_{(2)}H-C_{(1)}H$  group [Fig. 1(a)] is more concentrative on electron charges and can be easily attacked by ions or other polar molecules. The *s-gauche* conformer [Fig. 1(b)] provides a more explosive MEP for the terminal  $CH'$  group, which is out of the plane where three other carbon atoms reside. Any further rotation may reduce the maximized negative charge distribution of the terminal  $CH'$  group so as to increase the energy. It is further seen that the negative charge distribution of the terminal  $CH'$  group in the *s-gauche* conformer breaks into two isolated areas in the MEP of the saddle-point configuration, i.e., the *s-cis* conformer [Fig. 1(c)].

## B. Interconversion and coexistence of *s-trans/s-gauche*-1,3-butadiene

Torsional changes between *s-trans/s-gauche*-1,3-butadiene result in a very small energy variation, which produces the global and local minimum structures. Figure 2 compares the cross sections of the torsional potential-energy surfaces as a function of the torsional angle under the CC-CC single bond rotation, generated using the MP2/TZVP//MP2/TZVP and B3LYP/TZVP//MP2/TZVP models (the present work), a high-level *ab initio* calculation of the CCSD(T)/cc-pV5Z model of Karpfen and Parasuk,<sup>7</sup> and the derived experimental data of Engeln *et al.*<sup>13</sup> Note that the torsional angle  $\delta=0^\circ$  corresponds to the species which takes the *s-cis*-1,3-butadiene structure (i.e., the planar  $C_{2v}$  structure), whereas when  $\delta=180^\circ$  the species reaches the *s-trans*-1,3-butadiene structure. All the data in Fig. 2 were normalized to zero at the energy of *s-trans*-1,3-butadiene. In this figure, the potential-energy curve generated by the present MP2/TZVP model is in excellent agreement with

TABLE II. Comparison of energies for stationary structures on the 1,3-butadiene torsional potential-energy curves (energy in kcal/mol).

Model	$\Delta E_{tq}^a$	$\Delta E_{eb}^b$	Reference
MP2/TZVP	2.75	5.98	This work
B3LYP/TZVP	3.97	7.54	This work
MP2/6-31G*	2.68	...	41
G2	2.98 <sup>c</sup>	...	48
MP2/cc-pVTZ	2.89	6.50	7
B3LYP/cc-pVTZ	4.04	7.22	7
MP2/aug-cc-pVTZ	2.82	6.44	7
MP2/cc-pV5Z	2.90	6.50	7
CCSD(T)/cc-pV5Z	2.90	6.12	7
Expt. (UV)	2.93 <sup>d</sup>	...	3
Expt.	2.83	5.93	13
Expt. (Raman)	2.50	4.66	60

<sup>a</sup> $\Delta E_{tq}$  is the relative energy between *s-trans* and *s-gauche* 1,3-butadiene.

<sup>b</sup> $\Delta E_{eb}$  is the energy barrier between *s-trans* and *s-gauche* 1,3-butadiene.

<sup>c</sup> $\Delta\Delta H$  (298).

<sup>d</sup> $\Delta\Delta H$  (320).

experiment<sup>13</sup> and the high-level *ab initio* model of CCSD(T)/cc-pV5Z.<sup>7</sup> In the large torsional angle region of  $\delta > 50^\circ$ , the energy differences between that calculated using the present MP2/TZVP model and the experiment are almost indistinguishable until in the vicinity of the *s-gauche* conformer. In the low angular region ( $\delta < 50^\circ$ ), small energy discrepancies in the results are shown. It is noted that the DFT models consistently predicted higher *trans-gauche* barriers than the *ab initio* models,<sup>7</sup> which was also observed in Fig. 2.

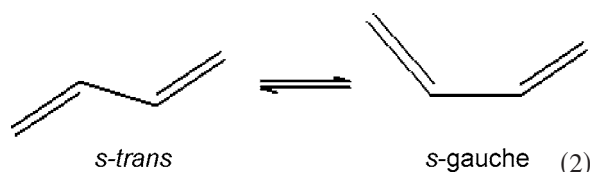
The energy differences and the energy barriers between the *s-trans/s-gauche* conformers are given in Table II. The CCSD(T)/cc-pV5Z model gave an energy barrier ( $\Delta E_{eb}$ ) between the *s-trans/s-gauche* conformers of 6.12 kcal/mol,<sup>7</sup> whereas the experimental barrier was estimated as 5.43 kcal/mol.<sup>13</sup> This property was calculated to be 5.98 and 7.54 kcal/mol using the MP2/TZVP and B3LYP/TZVP models, respectively, in present work. Such an energy barrier to the 1,3-butadiene conformer interconversion reaction is even smaller than those in the *s-cis-Z-s-cis*  $\rightarrow$  *s-trans-Z-s-cis*  $\rightarrow$  *s-trans-Z-s-trans* interconversion reactions of *Z*-1,3,5-hexatriene.<sup>47</sup> Therefore, it is possible for the *s-trans* and *s-gauche* 1,3-butadiene conformers to coexist. Table II also indicates that the energetics produced in the present calculations for the conformers are in excellent agreement with both theory and experiments. For example,  $\Delta E_{tq}$  is 2.75 kcal/mol from the MP2/TZVP model, which agrees well with the range of theoretical calculations of 2.3-4.0 kcal/mol (Ref. 7) with many of those values clustering close to 3.0 kcal/mol.<sup>7,42,48</sup> The present results are also in good agreement with a recent experimental enthalpy difference of  $\Delta H_{320}^0 = 2.93 \pm 0.01$  kcal/mol.<sup>3</sup> The energy barrier between the global and local minimum structures is only 5.98 kcal/mol by the MP2/TZVP//MP2/TZVP model and 7.54 kcal/mol by the B3LYP/TZVP//MP2/TZVP model in the present work, which agree well with the other work listed in Table II. The energy barriers between the *cZc-tZc* and *tZc-tZt* interconversion reactions of *Z*-1,3,5-hexatriene<sup>47</sup> are 7.50 and 7.20 kcal/mol, respectively. Hence, the *s-trans/*

TABLE III. Comparison of the vertical ionization energies (binding energy) of 1,3-butadiene with other theoretical and experimental studies (energy in eV).

MO	Symmetry	Theory					Experiment	
		SAOP/TZVP <sup>a</sup>		OVGF <sup>b</sup>	ADC(3) <sup>b</sup>	CI <sup>c</sup>	PES <sup>b</sup>	EMS <sup>d</sup>
		<i>s-trans</i>	<i>s-gauche</i>	<i>s-trans</i>	<i>s-trans</i>	<i>s-trans</i>		
1	$1b_g$	9.93	9.98	8.91	8.88(0.88)	9.29	9.29 <sup>e</sup>	9.20
2	$1a_u$	12.13	11.74	<sup>f</sup>	11.29(0.63)	12.10	11.48 <sup>g</sup>	11.50
3	$7a_g$	12.40	12.43	12.22	12.18(0.89)	12.98	12.20 <sup>g</sup>	12.20
4	$6b_u$	13.41	13.00	13.56	13.42(0.86)	14.43	13.49 <sup>g</sup>	13.40
5	$6a_g$	13.59	14.43	13.78	13.80(0.88)	14.50	13.90 <sup>g</sup>	13.90
6	$5a_g$	15.41	14.70	15.37	15.33(0.79)	16.24	15.30 <sup>g</sup>	15.50
7	$5b_u$	15.50	16.10	<sup>f</sup>	15.89(0.54)	16.55	15.80 <sup>g</sup>	15.50

<sup>a</sup>This work.<sup>b</sup>See Ref. 5.<sup>c</sup>See Ref. 52.<sup>d</sup>See Ref. 6.<sup>e</sup>The centroid of the photoelectron band (Ref. 5).<sup>f</sup>The OVGF is inapplicable because of strong many-body effects leading to intense satellite line structure. (Ref. 5).<sup>g</sup>The PES experiment gave approximate values (Ref. 5).

*s-gauche* conformers need only a small extra energy to achieve the photochemical interconversion,<sup>3,14,49</sup>



It is possible for the conformers to coexist under certain circumstances such as conformer-specific chemical reactions.<sup>3,49–51</sup> The barrier to rotation about the central bond is small and rotation to the less favorable, but reactive *s-cis* conformation is rapid.<sup>3</sup> Although the molar percentage for the *s-gauche* conformer is very small, the existence of the *s-gauche* conformer in the 1,3-butadiene sample makes it possible to induce the *s-trans/s-gauche* equilibrium [Eq. (2)] to move toward the product under certain conditions. For example, the reactions of addition of hydrogen halides (H X) to 1,3-butadiene indicate the domination of the *s-trans* conformer. Alternatively, the retro-Diels-Alder cycloaddition reactions, which are sterically restricted to take up the *gauche* (*cis*) conformation, provide evidence for *s-gauche* (*s-cis*) conformer domination. In the latter cases, the dynamical interconversion of *s-trans/s-gauche*, [Eq. (2)], moves towards the product side of the reaction. This photochemical interconversion allows both the *s-trans* and the *s-gauche* conformers to be characterized by IR and UV spectroscopy,<sup>3</sup> even though the molar fraction under room temperature ( $T = 298.53$  K) is dominated by *s-trans*-1,3-butadiene (94.79%) with only 5.21% for *s-gauche*-1,3-butadiene.

### C. Ionization energies of the conformers in outer valence space

The ground electronic states of the conformers have closed shells with 15 doubly occupied orbitals, respectively.

There are four core orbitals and four inner valence orbitals, the remaining seven orbitals are outer valence orbitals which are the focus of this study. The *s-trans*-1,3-butadiene ( $C_{2h}$ ) conformer possesses an  $X^1A_g$  ground electronic state, namely,

$$(1a_g)(1b_u)(2a_g)(2b_u)(3a_g)(3b_u)(4a_g)(4b_u)(5b_u)(5a_g) \\ \times (6a_g)(6b_u)(7a_g)(1a_u)(1b_g)$$

whereas the *s-gauche*-1,3-butadiene ( $C_2$ ) conformer has an  $X^1A$  ground state, namely,

$$(1a)(1b)(2b)(2a)(3a)(3b)(4a)(4b)(5a)(6a)(5b)(6b)(7a) \\ \times (7b)(8a).$$

Table III compares the vertical ionization energies of the outer valence orbitals for the global minimum structure of 1,3-butadiene, using the SAOP/TZ2P//B3LYP/TZVP model, together with other theoretical results using OVGF,<sup>5</sup> ADC(3)-GF,<sup>5</sup> and configuration interaction (CI) (Ref. 52) as well as the PES and EMS experimental data.<sup>5,6</sup> These ionization energies generated by the SAOP/TZ2P model have achieved an overall good agreement with the observed PES (Ref. 5) and EMS (Ref. 6) spectra. Theoretically, the SAOP/TZ2P model produced results which are more accurate, compared to those obtained by a CI calculation.<sup>5</sup> It seems that the CI model produced the outermost three orbitals, i.e.,  $1b_g$ ,  $1a_u$ , and  $7a_g$ , with a reasonable accuracy, however, large errors occurred in the other outer valence orbitals generated by the CI calculations as shown in this table. The present model (SAOP/TZ2P) could achieve a similar accuracy to the results obtained using the Green's Function (GF) calculations such as OVGF and ADC(3).<sup>5</sup> However, one initially needs to note that the experimental energies themselves were approximate results in this case. For example, the largest discrepancy between the PES and EMS experiments is 0.30 eV for orbital  $5b_u$ .<sup>5,6</sup> Second, the experimental data were averaged binding energies of all the possible conformers existing un-

TABLE IV. Comparison of the vertical ionization energies (binding energy) of 1,3-butadiene conformers using various theoretical models (energy in eV).

MO	RHF/TZVP				OVGF/TZVP		SAOP/TZ2P		Expt. (PES) <sup>a</sup>
	Symmetry	$\epsilon^b$	Symmetry	$\epsilon^{bc}$	$\epsilon^f$	$\epsilon^g$	$\epsilon^f$	$\epsilon^g$	
1	$1b_g$	8.82	$8a$	8.81	8.87(0.90)	9.04(0.91)	9.93	9.98	9.29
2	$1a_u$	12.11	$7b$	12.01	11.54(0.88)	11.20(0.89)	12.13	11.74	11.48
3	$7a_g$	13.48	$7a$	13.62	12.32(0.90)	12.36(0.90)	12.40	12.43	12.20
4	$6b_u$	14.86	$6b$	14.09	13.63(0.89)	13.14(0.90)	13.44	13.00	13.49
5	$6a_g$	15.26	$5b$	15.95	13.71(0.90)	13.78(0.88)	13.59	14.43	13.90
6	$5a_g$	17.36	$6a$	16.73	15.68(0.86)	14.99(0.89)	15.41	14.70	15.30
7	$5b_u$	17.60	$5a$	18.29	15.90(0.87)	16.54(0.85)	15.50	16.10	15.80

<sup>a</sup>See Ref. 5<sup>b</sup> $t$  for *s-trans*-1,3-butadiene.<sup>c</sup> $g$  for *s-gauche*-1,3-butadiene.

der the particular experimental conditions. The present calculations showed that the *s-gauche* conformer yields slightly different ionization energies, which could make some contribution to the observed ionization energies of 1,3-butadiene. The ADC(3) calculations resulted in ionization energies with a competitive accuracy with the SAOP model, but were computationally more expensive. However, the ADC(3) calculations suggested strong orbital electron correlation in those cases where the spectroscopic pole strengths were less than 0.80.<sup>38</sup> For example, the next-HOMO (NHOMO),  $1a_u$ , and the last outer valence orbital,  $5b_u$ , show strong electron correlation with the corresponding dominant pole strengths being 0.63 and 0.54, respectively,<sup>5</sup> as seen in Table III. This caused their OVGF method to fail to reproduce the ionization energies for these states.<sup>5</sup> Last, the orbitals with strong configuration interactions, such as orbitals  $1a_u$ ,  $5a_g$ , and  $5b_u$ , might receive a contribution from *s-gauche*-1,3-butadiene through the equilibrium [Eq. (2)]. For example, the SAOP/TZ2P results of *s-gauche*-1,3-butadiene give the ionization energies for orbitals  $7b$  and  $5b$  as 11.74 and 16.10 eV, respectively, which exhibit closer values to the corresponding experimental data of 11.48 and 15.80 eV,<sup>5</sup> than the pair of 12.13 and 15.50 eV of the *s-trans* structure. As a result, it is possible that the *s-gauche* conformer makes stronger contributions to those states than the others.

Table IV compares the ionization energies of the two conformers in their outer valence shell using *ab initio*, Green's function and DFT methods such as RHF/TZVP, OVGF/TZVP, and SAOP/TZ2P. As seen in this table, when the orbitals move inwards, the agreement between the RHF/TZVP model and experiment becomes poor. The other models, such as OVGF/TZVP and SAOP/TZ2P, which include a certain degree of electron correlation effects, do not seem to behave less accurately when one moves to the right-hand side of the binding-energy spectrum. This indicates that apart from the orbital relaxation effects, electron correlation effects are important for an accurate binding-energy prediction. The ionization energies of the conformers in the outer valence shell do not look very different from each other. However, the orbital symmetries of the conformers are certainly different and therefore, the molecular spectra (distributions of transition lines) of *s-gauche*-1,3-butadiene will not be the same as the *s-trans* conformer. This property from theory can

be used as a guideline to design a new experiment to differentiate the conformers.<sup>3,14,49</sup> Finally, the differences between the OVGF calculations of the present work and Ref. 5 need to be addressed. The two OVGF calculations agree generally well, but with small shifts in energy in the outer valence shell. The most apparent differences in the results between the OVGF calculations are (1) the present calculation produced all the orbitals in the outer valence shell with pole strengths within 0.86–0.90, indicating that the independent particle picture used in the later section is a valid approximation. (2) Only five outer valence orbitals out of seven were produced by the OVGF model in Ref. 5. In the present OVGF/TZVP calculations, which is based on the optimized geometry of the B3LYP/TZVP model, we used GAUSSIAN03 (Ref. 27) and the TZVP basis set, i.e., an OVGF/TZVP//B3LYP/TZVP model. The other OVGF calculations,<sup>5</sup> on the other hand, were based on the experimental geometry of Landolt-Bornstein,<sup>53</sup> and the basis sets in the calculations were modified from the atomic natural orbital basis set of Widmark *et al.*<sup>54</sup> In addition, their OVGF calculations were performed using the MOLCAS 2 package.<sup>55</sup>

#### D. Orbital correlations between *s-trans/s-gauche*-1,3-butadiene

The *s-gauche*-1,3-butadiene conformer can be considered as the result of torsional angle  $\delta$  changes from  $180^\circ$  to  $\approx 32.81^\circ$ . Figure 3 displays the ionization energy levels in the outer valence shell and demonstrates the relationship between the orbitals of the two minimum structures given in Figs. 1(a) and 1(b). As the conformers possess  $C_{2h}$  (*s-trans*) and  $C_2$  (*s-gauche*) symmetries, the principal  $C_2$  axis remains during the torsional motion. As a result, the block of symmetry-*a* orbitals and the block of symmetry-*b* orbitals do not mix in the matrix-diagonalizing process. Therefore, the numbers of orbitals with *a* and *b* symmetries in *s-trans*-1,3-butadiene must be the same as in the *s-gauche* conformer. The orbitals in the *s-trans/s-gauche* conformers are correlated by their symmetry and energies. Figure 3 reflects the symmetry and energy correlation of the pair. As the torsional angle  $\delta$  decreases from  $180^\circ$  to reach the local minimum at  $\delta=32.81^\circ$  (B3LYP/TZVP), almost all the outer valence orbitals of the pair experience energy shifts and/or



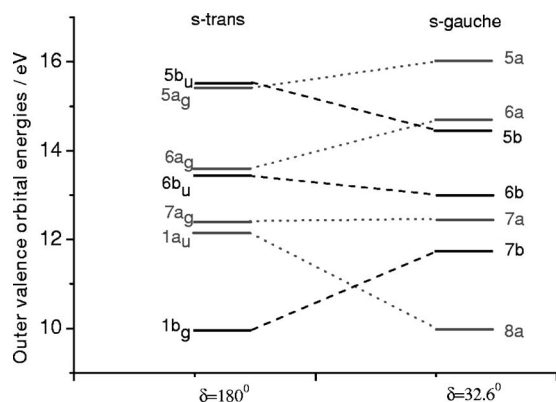


FIG. 3. Outer valence space-orbital energy correlation of the *s-trans/s-gauche*-1,3-butadiene conformers based on the SAOP/TZVP model.

symmetry flips except a couple of middle outer valence orbitals ( $7a_g$  and  $6b_u$ ).

In order to further explore the orbital correlation between the conformers, a set of three outermost frontier orbitals ( $1b_g$ ,  $1a_u$ , and  $7a_g$ ) is selected in the analysis. These three frontier orbitals reflect the orbital changes, such as crossing and remaining, and therefore can be considered as representatives of the outer valence orbitals of the conformer pair under study. Figure 4 exhibits the correlation of these outer valence orbitals accommodating with their electron charge distributions. It can be seen that for *s-trans*-1,3-butadiene, the HOMO ( $1b_g$ ) and NHOMO ( $1a_u$ ) are  $\pi$  bonds formed by the carbon  $2p_z$  atomic orbitals (AO) to a pair of double bonds in an antibonding fashion (HOMO), i.e., a node in the midpoint of the central C–C bond, and in a delocalized bonding fashion (NHOMO) to fulfill the conjugation. The molecular plane in which all the atoms reside serves as a nodal plane in the HOMO and NHOMO of this *s-trans* conformer. The 3rd orbital, labeled as  $7a_g$  in the left-hand side, however, demonstrates an in-plane bonding fashion of  $sp^2$  hybridization. The dominant  $2p_x$  and  $2p_y$  AOs of the four carbon atoms bond with the  $1s$  AOs of the hydrogen atoms. The middle carbon pair forms a  $\sigma$  bond by the  $sp^2$  orbitals in a head-on fashion. It is this orbital which is totally symmetric to the rotation of the central C–C bond of 1,3-butadiene. As a result, the torsional angle changes do not cause a significant

increase or reduction in the orbital electron density overlap and therefore, the energy of this orbital does not change obviously with the torsional angle  $\delta$ , which is seen in Fig. 4. However, the shape of the orbital wave functions has certainly been changed. This is demonstrated by the orbital MDs in a later section.

It seems that the HOMO ( $1b_g$ ) of *s-trans*-1,3-butadiene would correlate to the HOMO of the *s-gauche*-1,3-butadiene ( $8a$ ), whereas the NHOMO of the *s-trans*-1,3-butadiene ( $1a_u$ ) would correlate to the NHOMO of *s-gauche*-1,3-butadiene ( $7b$ ), since the electron charge distributions of the two pairs of HOMO-HOMO and NHOMO-NHOMO correlation appear to possess closer energies and exhibit similar patterns in wave functions. However, the orbital symmetry is violated for such correlations. The symmetry of the orbitals suggests that the HOMO ( $1b_g$ ) of the *s-trans* species correlates to the NHOMO ( $7b$ ) of the *s-gauche* conformer, and alternatively, the NHOMO ( $1a_u$ ) of the *s-trans* conformer links with the HOMO ( $8a$ ) in the *s-gauche* species. During the torsional changes from the *s-trans* to the *s-gauche* configuration, what remains unchanged is the  $C_2$  axis rather than the molecular plane or any other symmetry axes. Moreover, the  $C_2$  axis in the *s-gauche* conformer is perpendicular to the central C–C bond and lies in a plane (the  $xz$  plane) which contains the central C–C bond, but equally divides the dihedral angle of  $\angle(C_3C_1C_2C_4)$  ( $32.81^\circ$ ). By convention, the principal symmetric axis of a molecule is the  $z$  axis. As a result, the  $xz$  plane of the *s-gauche*-1,3-butadiene is formed by rotating  $16.4^\circ$  (half of the dihedral angle of  $32.81^\circ$ ) from the  $xy$  plane of the *s-trans*-1,3-butadiene. This observation is evident from the dipole moments of *s-gauche*-1,3-butadiene. That is, the totally symmetric *s-trans*-1,3-butadiene does not possess a permanent dipole moment, whereas the *s-gauche*-1,3-butadiene exhibits a small nonzero total dipole moment with  $\mu_z=0.098$  Debye,  $\mu_x=0$ , and  $\mu_y=0$  (B3LYP/TZVP).

## E. Calculated Dyson orbitals in $r$ -space and $k$ -space

The energies and other properties based on the  $C_{2h}$  and  $C_2$  point groups alone still convey limited information about the differences in electronic structure associated with each of the ionization energies.<sup>56</sup> As a result, Dyson orbitals of the conformers are calculated and analyzed in both coordinate  $r$ -space as orbital electron charge distributions (CDs) and in the momentum  $k$ -space as MDs. The latter could also be used to interpret and obtain insight and understanding into the EMS of 1,3-butadiene.<sup>6</sup>

Figure 5 gives the symmetry-correlated orbital MDs in the outer valence orbitals of the two minimum-energy structures of 1,3-butadiene. The seven outer valence orbitals of the conformer pair can be divided into two groups with group 1 consisting of MO4 ( $6b_u$  and  $6b$ ), MO5 ( $6a_g$  and  $6a$ ), and MO7 ( $5b_u$  and  $5b$ ), and group 2 consisting of MO1

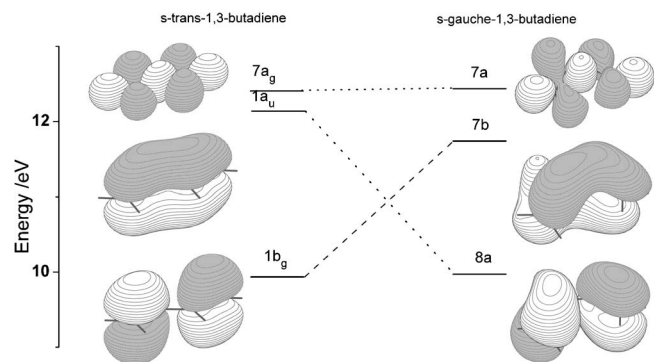


FIG. 4. The correlation between the outermost three valence orbitals of *s-trans/s-gauche*-1,3-butadiene based on the SAOP/TZVP model (energy) and the B3LYP/TZVP model (orbitals). The orbitals are plotted using MOLDEN (Ref. 61).

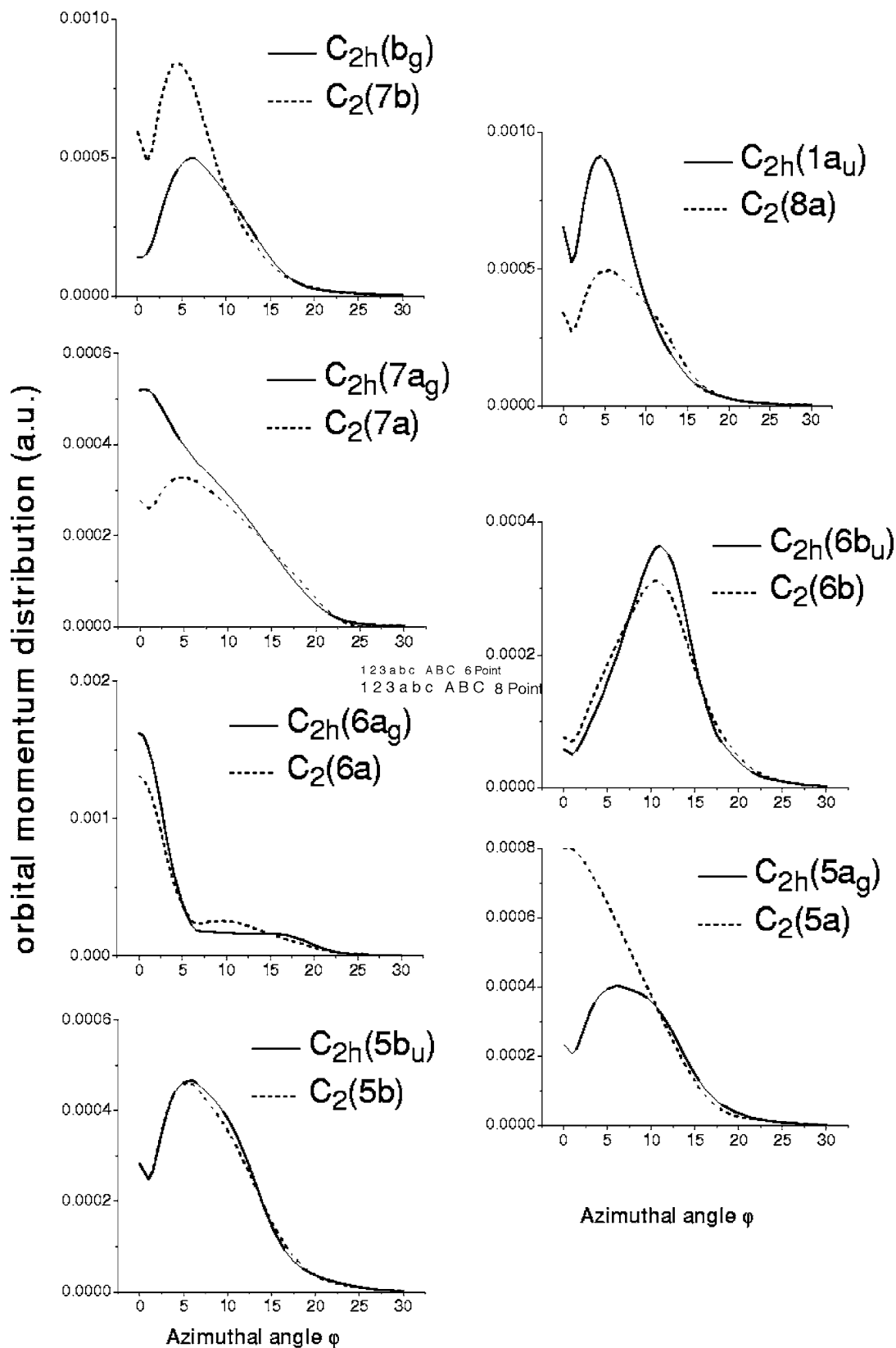


FIG. 5. The symmetry-correlated orbital momentum distributions of the outer valence orbitals of *s-trans/s-gauche*-1,3-butadiene based on the B3LYP/TZVP wave functions.

(HOMO,  $1b_g$  and  $7b$ ), MO2 (NHOMO,  $1a_u$  and  $8a$ ), MO3 ( $7a_g$  and  $7a$ ), and MO6 ( $5a_g$  and  $5a$ ). The torsional motion does not significantly change the orbital MDs for group 1

orbitals in this figure, suggesting the symmetric or antisymmetric nature along the C–C bond and forming in-plane  $\sigma$  bonds. The group 2 orbitals differentiate the changes in the

*s-trans/s-gauche* conformers, as they exhibit quite different orbital MDs in the conformer pair. Consequently, group 2 orbitals serve as the *gauche* conformer signatures. In MO1 (HOMO,  $1b_g$  and  $7b$ ) and MO6 ( $5a_g$  and  $5a$ ) the orbital MDs of the *s-trans* conformer (solid lines) lie below the orbital MDs of the *s-gauche* conformer (dash lines), whereas in MO2 (NHOMO,  $1a_u$  and  $8a$ ) and MO3 ( $7a_g$  and  $7a$ ), the orbital MDs of the *s-trans* conformer lie above the *s-gauche* conformer. The HOMO and NHOMO in the *s-trans* conformer contain a nodal plane as the molecular plane, suggesting  $\pi$  bonds formed by the carbon  $2p_z$  AOs, which contribute to the conjugation  $\pi$ -bond system of butadiene. For example, the HOMO of the *s-trans* conformer gives the  $C_{(3)}=C_{(1)}$  and  $C_{(2)}=C_{(4)}$   $\pi$  bonds (HOMO, see Fig. 4 for the orbital electron charge density), while the NHOMO contributes to the delocalized extended  $\pi$  bond connecting four carbon atoms. Such natures of the HOMO and NHOMO in the *s-trans* conformer do not experience significant changes, but are swapped in the *s-gauche* conformer, as indicated by their orbital MDs quantitatively in Fig. 5. In addition, MO3 and MO6 are indicators of the torsional changes on the affected orbitals of the central C–C bond, which were observed previously in *n*-butane.<sup>21</sup>

It is possible that configurations of the minimum-energy structures were very competitive and could undergo interconversion in the EMS experimental conditions,<sup>6</sup> as a result of the coexistence of *s-trans/s-gauche*-1,3-butadiene. Figure 6 compares the synthesized orbital momentum distributions of the outer valence orbitals of the 1,3-butadiene conformer pair with the EMS experiment.<sup>6</sup> The EMS spectra in momentum space can be divided into individually observed orbitals, such as the outermost three orbitals of MO1, MO2, and MO3, and unresolved orbitals such as MO4+MO5 and MO6+MO7. This figure suggests that the experimental orbital MDs (cross sections) might have observed the orbitals of interchangeable conformers in various binding-energy regions in the spectra. For example, in the individually resolved outermost three valence orbitals, it is clear that the HOMO is dominated by *s-trans*-1,3-butadiene, the global minimum structure, whereas the NHOMO and MO3 seem to be dominated by the  $8a$  and  $7a$  orbitals (dot lines) of the *s-gauche*-1,3-butadiene conformer, respectively. Moreover, the HOMO (the solid line in the  $1b_g$  orbital) of the *s-trans* conformer agrees apparently well with the EMS experiment under the experimental conditions.<sup>6</sup> The good agreement in the orbital MDs of the HOMO ( $1b_g$ ) indicates that the B3LYP/TZVP model in the present work is a more accurate model than those employed in the earlier simulation.<sup>6</sup> Due to the symmetry, when *s-trans*-1,3-butadiene experiences torsional changes, the symmetry channel of the HOMO ( $1b_g$ ) in the  $C_{2h}$  conformer could not lead to the HOMO ( $8a$ ) but to the NHOMO ( $7b$ ) of the *s-gauche* conformer, although the  $1b_g$  orbital is closer to the  $8a$  orbital of the *s-gauche* species in energy.

The torsional changes also lead the NHOMO ( $1a_u$ ) of the *s-trans* species to become the HOMO ( $8a$ ) of the *s-gauche* species, which is more symmetrically and energetically viable. The agreement of the  $8a$  orbital of the *s-gauche* conformer to the experimental MD is excellent. The third outer valence orbitals of *s-trans* ( $7a_g$ ) and *s-gauche* ( $7a$ ) are

competitive in energy. As a resolved orbital in the outer valence space, this  $7a$  orbital of the *s-gauche* conformer (dot line) in Fig. 6 agrees very well (within the error bars) with the experiment, much better than the orbital ( $7a_g$ ) of the *s-trans* conformer (solid line). The second orbital MDs in this figure, i.e., MO2, is related to orbital  $8a$  which has the lowest binding energy—the “HOMO” of the *s-gauche*-1,3-butadiene conformer. As indicated in Fig. 4, due to the lower orbital energy (9.98 eV) of the *s-gauche* structure than the corresponding orbital ( $1a_u$ ) energy (12.13 eV) of the *s-trans* configuration, it is possible under the experimental conditions that the conformers interchange towards the local minimum structure in this orbital channel. The strong electron correlation predicted by the many-body GF method<sup>5</sup> supported the above interpretation. The MO3 case, on the other hand, is obviously a competition between the pair conformers, as both the orbital energies of the conformers, 12.40 eV for  $7a_g$  and 12.43 eV for  $7a$ , are close in value. This competition results in the orbital of the *s-gauche* conformer ( $7a$ , dot line), which is within the experimental error bars as indicated in Fig. 6 without any scaling. There do not exist any outer valence orbitals in this envelope of peak 3 in the binding-energy spectra<sup>6</sup> which exhibit the shape given by the EMS experiment for *s-trans*-butadiene, again indicating the existence of conformers. The PWIA-SCF and PWIA-DFT(LDA) of Snyder *et al.*<sup>57</sup> with TZ94P basis sets in the earlier simulation<sup>6</sup> produced the correct information for *s-trans* conformer of 1,3-butadiene, while the other set of basis sets including the same TZVP basis set as employed in this work, in fact, generated the orbital of the *s-gauche* conformer. Note that the dash lines in MO3 and MO6+MO7 in Fig. 6 are not orbital MDs, but indicate a certain symmetry of the corresponding  $C_{2h}$  and  $C_2$  orbitals.

Due to the experimental resolution (ca. 1.60 eV),<sup>58</sup> it is quite difficult to individually resolve orbitals  $6b_u$  (ca. 13.40 eV) and  $6a_g$  (ca. 13.90 eV), as well as orbitals  $5a_g$  (ca. 15.50 eV) and  $5b_u$  (ca. 15.50 eV). The unresolved experimental orbital MD pairs, however, exhibit very diverse shapes for the combined orbital MD pairs. The orbital MDs corresponding to peak 4 of the binding-energy spectra<sup>6</sup> are likely to result from the superposition of orbitals  $6b_u$  and  $6a_g$  of the *s-trans* conformer (MO4+5 in Fig. 6). The last combined orbital MDs in the outer valence space, which correspond to peak 5 of the same binding-energy spectra, in fact, seem to be a superposition of the  $5b+5a$  orbitals of the *s-gauche* conformer as given in Fig. 6. It is noted, however, as indicated by Wang,<sup>17</sup> that the unresolved experimental orbital MDs provide only the behavior of the component orbitals collectively. As a result, detailed information of individual orbitals may be masked by the poor energy resolution and this causes information loss. For example, with the MO4+MO5 and MO6+MO7 pairs in Fig. 6, the collected behavior of the orbital MDs looks very different. Both of the pair orbitals are a superposition of two orbitals with one *a* symmetry and one *b* symmetry, though the former pair is dominated by the *s-trans* conformer and the latter is dominated by the *s-gauche* conformer.

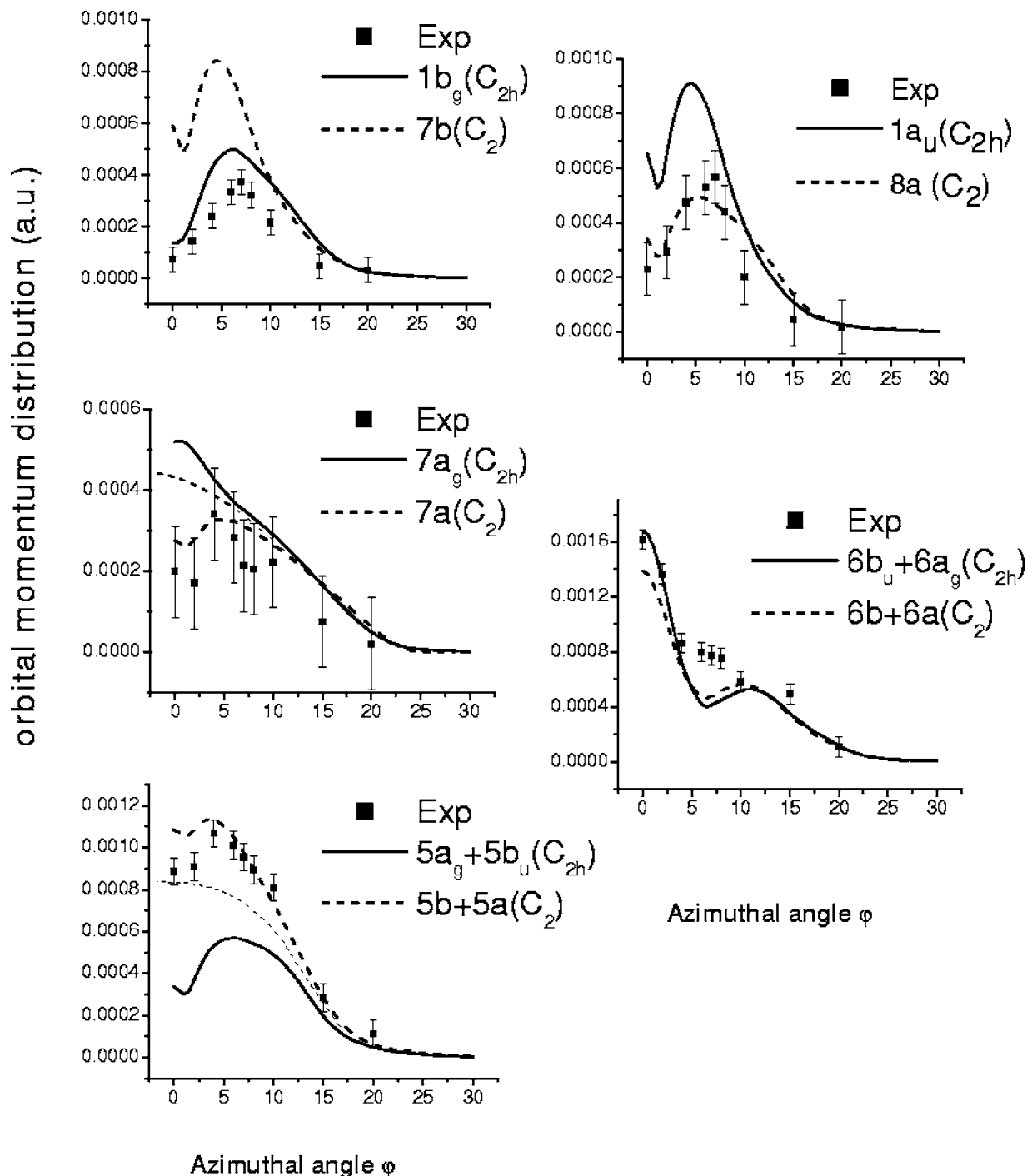


FIG. 6. A comparison of the experimental cross sections with the synthetic orbital momentum distributions of the outer valence orbitals (symmetry correlated) of the *s-trans/s-gauche*-1,3-butadiene based on the B3LYP/TZVP model. Note that the dashed lines in MO3 and MO6+7 are extensions of the orbital MDs from larger momentum regions as certain "symmetry axis."

To further explore related information for a more detailed understanding, we move one step forward to investigate the individual orbitals within the unresolved orbital pairs theoretically. Figure 7 compares the synthetic orbital MDs with the EMS experiment, together with the individual orbital MDs of orbitals  $6b_u$  and  $6a_g$  of *s-trans*-1,3-butadiene, whereas Fig. 8 provides the orbital MDs for the combined orbital pair of  $5b+5a$  as well as the individual orbital MDs of orbitals  $5b$  and  $5a$  of the local minimum structure of *s-gauche*-1,3-butadiene. It is seen from the orbital MDs in

these figures that the corresponding individual orbitals, i.e.,  $6b_u$  vs  $5b$ ,  $6a_g$  vs  $5a$ , have certain similarities. The *b* orbitals concentrate on the C=C double bonds of 1,3-butadiene, whereas the *a* orbitals exhibit strong overlap in the C-C central bond region. As a result, the orbitals of *b* symmetry, i.e.,  $6b_u$  and  $5b$ , indicate an antibonding nature and with contributions from the carbon  $2p_z$  orbitals as shown by the dash lines in Figs. 7 and 8. The orbitals of *a* symmetry,  $6a_g$  and  $5a$ , show strong overlap along the carbon framework and involvement of the hydrogen atoms, with a bonding nature



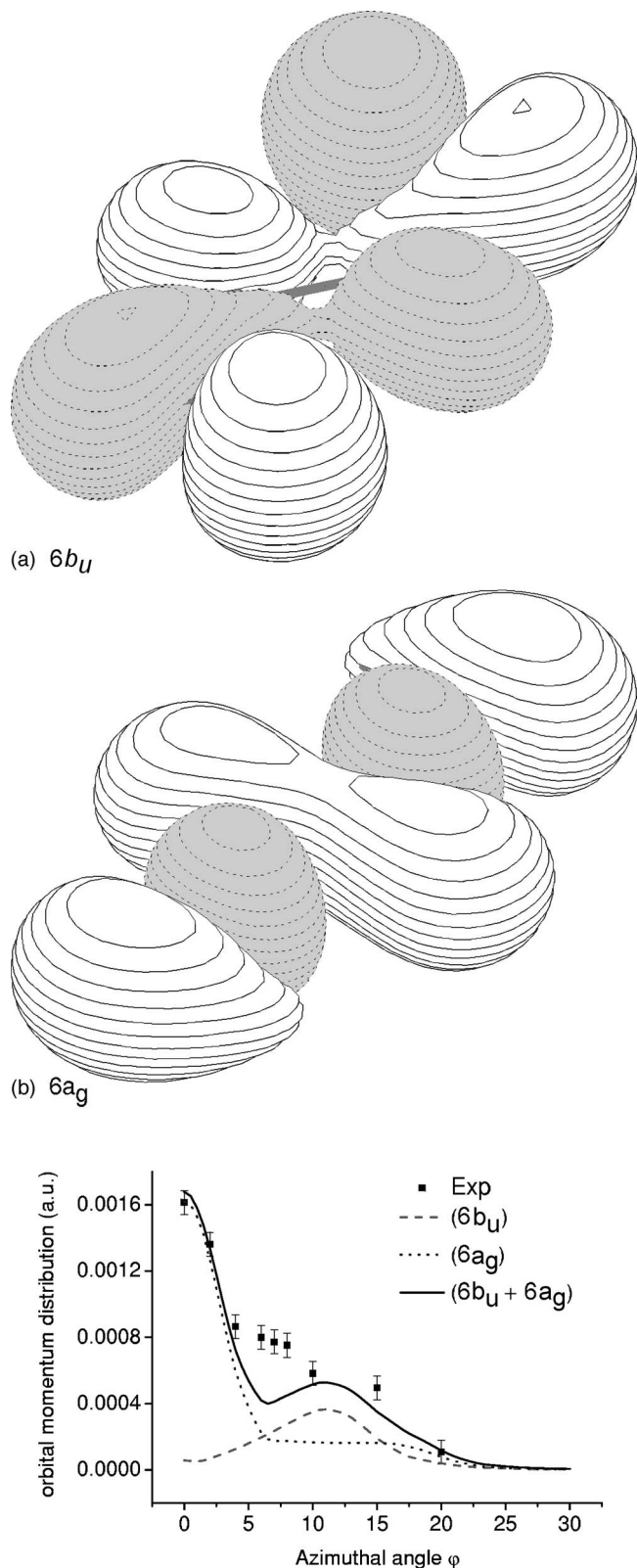


FIG. 7. Synthesis of the experimentally unresolved orbital momentum distributions of orbitals pairs of  $6b_u + 6a_g$  (*s-trans*-1,3-butadiene) based on the B3LYP/TZVP model. The orbital electron charge densities are plotted using MOLDEN (Ref. 61).

and with strong in-plane  $sp^x$  hybridization (dot lines in Figs. 7 and 8). However, as indicated by the solid lines in Figs. 7 and 8, the orbital pairs  $6b_u + 6a_g$  and  $5b + 5a$  look quite different collectively.

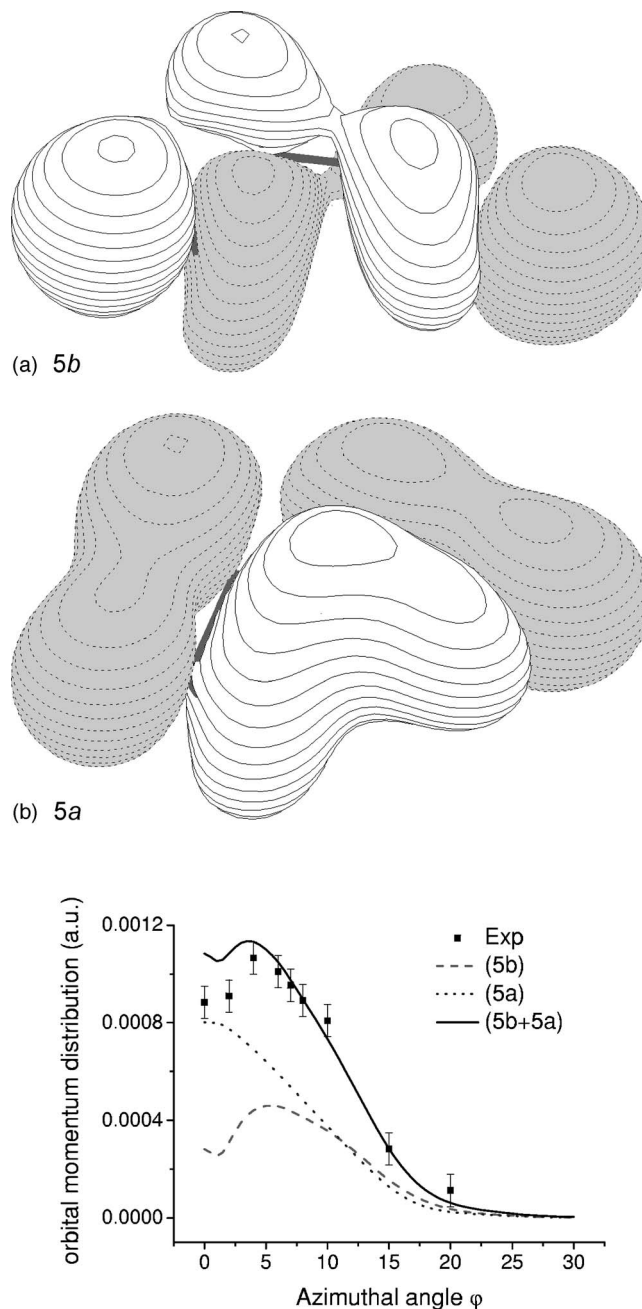


FIG. 8. Synthesis of the experimentally unresolved orbital momentum distributions of orbitals pairs of  $5b + 5a$  (*s-gauche*-1,3-butadiene) based on the B3LYP/TZVP model. The orbital electron charge densities are plotted using MOLDEN (Ref. 61).

#### IV. CONCLUSIONS

The outer valence space of the minimum-energy structures of 1,3-butadiene has been studied using a range of quantum-mechanical methods, including *ab initio* RHF and MP2 methods, a Green's function method (OVGF), and a couple of density-functional theory methods including B3LYP and the more recent SAOP. The most stable and second most stable structures of 1,3-butadiene are the planar *s-trans*-1,3-butadiene ( $C_{2h}$ ), and *s-gauche*-1,3-butadiene ( $C_2$ ), respectively. These findings agree with a number of other theoretical studies and experiments. The energy difference between the two structures is in fact very small: 3.97

and 2.75 kcal/mol, using the B3LYP/TZVP and MP2/TZVP models, respectively, which agree well with the believed range of 2.3–3.5 kcal/mol,<sup>42,48,59</sup> and the experimental energy of 2.93 kcal/mol.<sup>3</sup> A small and competitive energy barrier from the local minimum well [5.98 kcal/mol obtained using the MP2 model, which agrees well with the experimental value of 5.93 kcal/mol (Ref. 13)] makes it possible to interconvert between the conformers at the experimental conditions. As a result, the orbital momentum distributions observed with electron momentum spectroscopy were likely to be a mixture of distributions for a mixture of orbitals of *s-trans/s-gauche*-1,3-butadiene in the outer valence shell.

The interconversion of the conformers with slightly different orbital energy levels in the outer valence space may have caused problems with the assignment of peaks in previous photoelectron<sup>5</sup> and EMS<sup>6</sup> studies, with the EMS results being further complicated by unresolved peaks in their binding-energy spectra (BES). This is similar to the uncertainties that the mixture of the conformers caused in the interpretation of an electron-diffraction experiment.<sup>46</sup> The binding energies (ionization energies) of the species calculated using RHF, OVGf, and SAOP models have shown that the DFT SAOP model exhibits a competitive accuracy to that of the ADC(3) Green's function model, but with cheaper computational costs. The SAOP/TZ2P model gives generally better binding energies than the CI result<sup>52</sup> and the OVGf model. Furthermore, the Dyson orbitals of the conformers generated using the B3LYP/TZVP model and the plane-wave impulse approximation (PWIA) have been transformed into momentum space, where the respective orbital momentum distributions were compared with the EMS experimental measurement results on an individual orbital basis. Our results demonstrated again in momentum space that four out of the seven outer valence orbitals of the species are in fact engaged with *s-gauche*-1,3-butadiene, and three of such orbitals receive contributions from *s-trans*-1,3-butadiene. Such a finding further indicates the coexistence of the 1,3-butadiene conformer pair. The present work also leads to an understanding of why the stability of the planarity and *gauche* forms of 1,3-butadiene has long been a battle between both theoretical and experimental studies. It additionally provides more theoretical insight into the well-known organic addition reactions of 1,3-butadiene, which take the *s-trans* conformer in reactions such as the addition of hydrogen halides and the *s-gauche* conformers in reactions such as the retro-Diels-Alder reactions.

## ACKNOWLEDGMENTS

This research is partially supported by the Australian Research Council (ARC) and a Vice-Chancellor's Research Strategic Initiative Grant of Swinburne University of Technology. The authors acknowledge the Australian Partnership for Advanced Computing (APAC) for using the National Supercomputing Facilities. Finally, Professor M. S. Deleuze is thanked for drawing our attention to this issue.

<sup>1</sup>R. L. Melnick and M. C. Kohn, *Carcinogenesis* **16**, 157 (1995).

<sup>2</sup>A. Salomon, D. Cahen, S. Lindsay, J. Tomfohr, V. B. Engelkes, and C. D. Frisbie, *Adv. Mater. (Weinheim, Ger.)* **15**, 1881 (2003).

- <sup>3</sup>J. Saltiel, D. F. Sears, Jr., and A. M. Turek, *J. Phys. Chem. A* **105**, 7569 (2001).
- <sup>4</sup>K. T. Lee, J. Sung, K. J. Lee, S. K. Kim, and Y. D. Park, *Chem. Phys. Lett.* **368**, 262 (2003).
- <sup>5</sup>D. M. Holland, M. A. MacDonald, M. A. Hayes, P. Baltzert, B. Wannberg, M. Lundqvist, and W. von Niessen, *J. Phys. B* **29**, 3091 (1996).
- <sup>6</sup>M. J. Brunger, D. A. Winkler, M. T. Michalewicz, and E. Weigold, *J. Chem. Phys.* **108**, 1859 (1998).
- <sup>7</sup>A. Karpfen and V. Parasuk, *Mol. Phys.* **102**, 819 (2004).
- <sup>8</sup>L. Radom and J. A. Pople, *J. Am. Chem. Soc.* **92**, 4278 (1970).
- <sup>9</sup>D. Feller and E. R. Davidson, *Theor. Chim. Acta* **68**, 57 (1968).
- <sup>10</sup>N. L. Allinger, J. T. Fermann, W. D. Allen, and H. F. Schaefer III, *J. Chem. Phys.* **106**, 5143 (1997).
- <sup>11</sup>A. Almenningen and M. Traetteburg, *Acta Chem. Scand.* (1947-1973) **12**, 1221 (1958).
- <sup>12</sup>K. Kuchitsu, T. Fukuyama, and Y. Morino, *J. Mol. Struct.* **1**, 463 (1968).
- <sup>13</sup>R. Engeln, D. Consalvo, and J. Reuss, *Chem. Phys.* **160**, 427 (1992).
- <sup>14</sup>M. E. Squillacote, R. S. Sheridan, O. L. Chapman, and F. A. Anet, *J. Am. Chem. Soc.* **101**, 3657 (1979).
- <sup>15</sup>F. Dong and R. E. Miller, *Science* **298**, 1227 (2002).
- <sup>16</sup>S. Saha, F. Wang, and M. J. Brunger, <http://eccc.monmouth.edu/cgi-bin/discus/discus.cgi>.
- <sup>17</sup>F. Wang, *J. Phys. Chem. A* **107**, 10199 (2003).
- <sup>18</sup>A. Messiah, *Quantum Mechanics* (Wiley, New York, 1966).
- <sup>19</sup>J. J. Rehr and R. C. Albers, *Rev. Mod. Phys.* **72**, 621 (2000).
- <sup>20</sup>E. Weigold and I. E. McCarthy, *Electron Momentum Spectroscopy* (Kluwer-Academic, Dordrecht, 1999).
- <sup>21</sup>M. Downton and F. Wang, *Chem. Phys. Lett.* **384**, 144 (2004).
- <sup>22</sup>F. Wang and M. Downton, *J. Phys. B* **37**, 557 (2004).
- <sup>23</sup>F. Wang, *J. Mol. Struct.: THEOCHEM* **728**, 31 (2005).
- <sup>24</sup>F. Wang, M. Downton, and N. Kidwani, *J. Theor. Comput. Chem.* **4**, 247 (2005).
- <sup>25</sup>N. Godbout, D. Salahub, J. Andzelm, and E. Wimmer, *Can. J. Chem.* **70**, 560 (1992).
- <sup>26</sup>M. W. Schmidt, K. K. Baldrige, J. A. Boatz *et al.*, *J. Comput. Chem.* **14**, 1347 (1993).
- <sup>27</sup>M. J. Frisch, G. W. Trucks, H. B. Schlegel *et al.*, GAUSSIAN03, Revision C.02, Gaussian, Inc., Wallingford, CT, 2004.
- <sup>28</sup>J. J. Fisher and J. Michl, *J. Am. Chem. Soc.* **109**, 1056 (1987).
- <sup>29</sup>D. P. Chong, O. V. Gritsenko, and E. Baerends, *J. Chem. Phys.* **116**, 1760 (2002).
- <sup>30</sup>O. V. Gritsenko, B. Braida, and E. J. Baerends, *J. Chem. Phys.* **119**, 1937 (2003).
- <sup>31</sup>O. V. Gritsenko and E. J. Baerends, *J. Chem. Phys.* **117**, 9154 (2002).
- <sup>32</sup>D. P. Chong and C. Bureau, *J. Electron Spectrosc. Relat. Phenom.* **106**, 1 (2000).
- <sup>33</sup>O. Gritsenko, R. van Leeuman, and E. J. Baerends, *J. Chem. Phys.* **101**, 8955 (1994).
- <sup>34</sup>O. Gritsenko, R. van Leeuman, and E. J. Baerends, *Phys. Rev. A* **52**, 1870 (1995).
- <sup>35</sup>O. Gritsenko, P. Schipper, and E. J. Baerends, *Chem. Phys. Lett.* **302**, 199 (1999).
- <sup>36</sup>E. J. Baerends, J. Autschbach, A. Brces, C. Bo, P. M. Boerrigter, L. Cavallo, and D. P. Chong, ADF2004.01, SCM, Vrije Universiteit, Amsterdam, The Netherlands, Version 03, 2003; <http://www.scm.com>
- <sup>37</sup>D. P. Chong, E. V. Lenthe, S. van Gisbergen, and E. J. Baerends, *J. Comput. Chem.* **25**, 1030 (2004).
- <sup>38</sup>O. Dolgounitcheva, V. G. Zakrzewski, and J. V. Ortiz, *J. Am. Chem. Soc.* **122**, 12304 (2000).
- <sup>39</sup>P. Duffy, D. P. Chong, M. E. Casida, and D. R. Salahub, *Phys. Rev. A* **50**, 4707 (1994).
- <sup>40</sup>J. Breulet, T. J. Lee, and H. F. Schaefer, *J. Am. Chem. Soc.* **106**, 6250 (1984).
- <sup>41</sup>Y. N. Panchenko, J. V. Auwera, Y. Moussaoui, and G. R. D. Mare, *Struct. Chem.* **14**, 337 (2003).
- <sup>42</sup>H. Guo and M. Karplus, *J. Chem. Phys.* **94**, 3679 (1991).
- <sup>43</sup>E. Kraka, A. Wu, and D. Cremer, *J. Phys. Chem. A* **107**, 9008 (2003).
- <sup>44</sup>W. H. Haugen and M. Traetteberg, *Acta Chem. Scand.* (1947-1973) **20**, 1726 (1966).
- <sup>45</sup>K. Kuchitsu, T. Fukuyama, and Y. Morino, *J. Mol. Struct.* **4**, 41 (1969).
- <sup>46</sup>K. Kveseth, R. Seip, and D. A. Kohl, *Acta Chem. Scand., Ser. A* **A34**, 31 (1980).
- <sup>47</sup>D. Henseler, R. Rebertisch, and G. Hohlneicher, *Int. J. Quantum Chem.* **72**, 295 (1999).

- <sup>48</sup>M. A. Murcko, H. Castejon, and K. B. Wiberg, *J. Phys. Chem.* **100**, 16162 (1996).
- <sup>49</sup>B. R. Arnold, V. Balaji, and J. Michl, *J. Am. Chem. Soc.* **112**, 1808 (1990).
- <sup>50</sup>R. Srinivasan, *J. Am. Chem. Soc.* **90**, 4498 (1968).
- <sup>51</sup>S. Boue and R. Srinivasan, *J. Am. Chem. Soc.* **92**, 3226 (1970).
- <sup>52</sup>G. Fronzoni, P. Decleva, A. Lisini, and G. D. Alti, *J. Electron Spectrosc. Relat. Phenom.* **69**, 207 (1994).
- <sup>53</sup>In *Structure Data of Free Polyatomic Molecules*, Landolt-Bornstein New Series II Vol. 7, edited by K.-H. Hellwege and A. M. Hellwege (Springer, Berlin, 1976), p. 395.
- <sup>54</sup>P. O. Widmark, P. A. Malmqvist, and B. O. Roos, *Theor. Chim. Acta* **77**, 291 (1990).
- <sup>55</sup>K. Andersson, M. Barysz, A. Bernhardsson *et al.*, <http://www.teokem.lu.se/molcas/>
- <sup>56</sup>B. Herrera, O. Dolgounitcheva, V. G. Zakrzewski, A. Toro-Labbe, and J. V. Ortiz, *J. Phys. Chem. A* **108**, 11703 (2004).
- <sup>57</sup>L. C. Snyder, H. Bash, Z. R. Wasserman, and M. E. Baldacchino-Dolan, *Molecular Wave Functions and Properties: Tabulated from SCF calculations on a Gaussian Basis Set* (Wiley, New York, 1972).
- <sup>58</sup>M. Brunger and W. Adcock, *J. Chem. Soc., Perkin Trans. 2* **2002**, 1 (2002).
- <sup>59</sup>A. Karpfen, C. H. Choi, and M. Kertesz, *J. Phys. Chem.* **101**, 7426 (1997).
- <sup>60</sup>L. A. Carreira, *J. Chem. Phys.* **62**, 3851 (1975).
- <sup>61</sup>G. Schaftenaar and J. Noordik, *J. Comput.-Aided Mol. Des.* **14**, 123 (2000).